Title

A new streaked soft x-ray imager for the National Ignition Facility

Journal
Review of Scientific Instruments, 87(5)

ISSN
0034-6748

Authors
Benstead, J
Moore, AS
Ahmed, MF
et al.

Publication Date
2016-05-01

DOI
10.1063/1.4951689

Peer reviewed

A new streaked soft x-ray imager for the National Ignition Facility

J. Benstead, A. S. Moore, M. F. Ahmed, J. Morton, T. M. Guymer, R. Soufli, T. Pardini, R. L. Hibbard, C. G. Bailey, P. M. Bell, S. Hau-Riege, M. Bedzyk, M. J. Shoup, S. Reagan, T. Agliata, R. Jungquist, D. W. Schmidt, L. B. Kot, W. J. Garbett, M. S. Rubery, J. W. Skidmore, E. Gullikson, and F. Salmassi

Citation: Review of Scientific Instruments **87**, 055110 (2016); doi: 10.1063/1.4951689
View online: https://doi.org/10.1063/1.4951689
View Table of Contents: http://aip.scitation.org/toc/rsi/87/5
Published by the American Institute of Physics

REVIEW OF SCIENTIFIC INSTRUMENTS **87**, 055110 (2016)

A new streaked soft x-ray imager for the National Ignition Facility

J. Benstead,[1,a)] A. S. Moore,[2] M. F. Ahmed,[2] J. Morton,[1] T. M. Guymer,[1] R. Soufli,[2] T. Pardini,[2] R. L. Hibbard,[2] C. G. Bailey,[2] P. M. Bell,[2] S. Hau-Riege,[2] M. Bedzyk,[3] M. J. Shoup III,[3] S. Reagan,[3] T. Agliata,[3] R. Jungquist,[3] D. W. Schmidt,[4] L. B. Kot,[4] W. J. Garbett,[1] M. S. Rubery,[1] J. W. Skidmore,[1] E. Gullikson,[5] and F. Salmassi[5]
[1]*AWE, Aldermaston, Reading, Berkshire RG7 4PR, United Kingdom*
[2]*Lawrence Livermore National Laboratory, Livermore, California 94550, USA*
[3]*Laboratory for Laser Energetics, University of Rochester, Rochester, New York 14623, USA*
[4]*Los Alamos National Laboratory, Los Alamos, New Mexico 87545, USA*
[5]*Lawrence Berkeley National Laboratory, Berkeley, California 94720, USA*

(Received 5 January 2016; accepted 28 April 2016; published online 27 May 2016)

A new streaked soft x-ray imager has been designed for use on high energy-density (HED) physics experiments at the National Ignition Facility based at the Lawrence Livermore National Laboratory. This streaked imager uses a slit aperture, single shallow angle reflection from a nickel mirror, and soft x-ray filtering to, when coupled to one of the NIF's x-ray streak cameras, record a 4× magnification, one-dimensional image of an x-ray source with a spatial resolution of less than 90 μm. The energy band pass produced depends upon the filter material used; for the first qualification shots, vanadium and silver-on-titanium filters were used to gate on photon energy ranges of approximately 300–510 eV and 200–400 eV, respectively. A two-channel version of the snout is available for x-ray sources up to 1 mm and a single-channel is available for larger sources up to 3 mm. Both the one and two-channel variants have been qualified on quartz wire and HED physics target shots. [http://dx.doi.org/10.1063/1.4951689]

I. INTRODUCTION

Many HED experiments fielded on the NIF require accurate timing of the propagation of radiation through the target material in order to be properly diagnosed.[1] A number of diagnostics have already been developed for deployment on the NIF for this purpose,[2,3] but specific photon energy band pass, temporal, and spatial resolution requirements demanded by a number of experimental campaigns have led to the development of a new streaked soft x-ray imager; the S600-D (Streaked-600 mm-DISC). These requirements include imaging x-ray emission in relatively narrow band passes (≈±50 eV FWHM) in the soft x-ray region (<600 eV), continuous streaked recording over either 10 or 20 ns, less than 50 ps temporal resolution, and less than 90 μm FWHM spatial resolution. The S600-D is combined with one of the NIF's DISC (Diagnostic instrument manipulator Imaging Streak Camera) diagnostics.[4] Figure 1 shows a schematic of the S600-D design.

II. INSTRUMENT DESIGN

The S600-D is a diagnostic snout, which may be fielded on either the (northern) polar ($\theta = 0°$, $\phi = 0°$) or equatorial ($\theta = 90°$, $\phi = 78°$) DIM (Diagnostic Instrument Manipulator) on the NIF.[5]

It consists of a narrow aperture slit at the end closest to TCC (target chamber center) which acts as a pin hole in one spatial dimension. The standoff of this aperture from the emitting region of the target under observation is 150 mm and the distance from the aperture to the DISC detector is 600 mm, giving a 4× magnification of the target onto the imaging plane (in addition to the internal magnification of the DISC; typically 1.2×). The usable length of the DISC's photocathode slit varies between cameras, but is roughly 20 mm, allowing a 5 mm sized region to be imaged. Budgeting for diagnostic pointing errors up to ±1 mm reduces the maximum source size to approximately 3 mm.

For smaller source sizes of 1 mm and below, a two-channel variant of the diagnostic also exists. This design uses two aperture slits, which may be of differing sizes, to produce two side-by-side images on the photocathode. Restricting the source size to 1 mm for a two-channel measurement prevents any overlap or clipping of the two images. The nickel mirror pack also differs between the two variants. The single-channel pack has a single mirror with a central angle of 4.249° relative to the central axis of the snout and the two-channel pack has two mirrors, each angled at 4.120°. Depending upon the pointing of the snout and x-ray source size a range of scattering angles between 3.7° and 5.3° is expected.

Within the snout, x-rays passing through the aperture travel first through a (currently unused) forward filter basket, then undergo grazing angle reflection from a nickel mirror, pass through an x-ray filter located in the snout's kinematic base, and then land on the photocathode. Stray x-rays are blocked by collimators throughout the snout and hard x-rays are blocked by a direct line-of-sight tungsten shield which sits between the nickel mirror(s) and TCC. The engineering design and manufacture of the snout were performed by the

a)Electronic mail: james.benstead@awe.co.uk

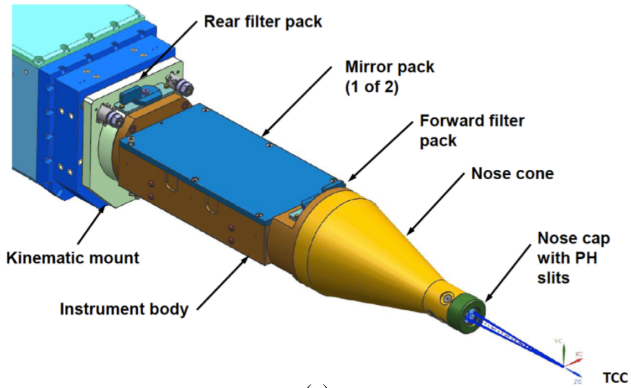

(a)

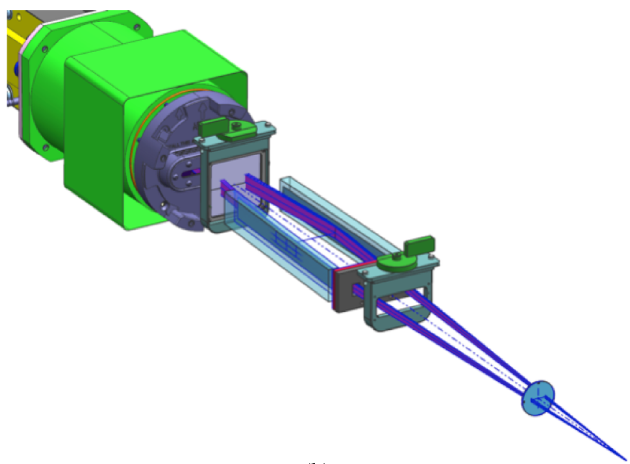

(b)

FIG. 1. The S600-D snout. (a) Schematic with important features highlighted. (b) Schematic of the light paths taken through the internal components in a two-channel configuration. The tungsten line-of-sight shield is visible in grey behind the forward filter basket.

Laboratory for Laser Energetics' Mechanical Engineering group in collaboration with the NIF Target Diagnostics Engineering group.

A. Mirror

Nickel was chosen as the mirror coating material due to its relatively "flat" reflectivity versus photon energy response for x-rays across both the energy region of interest and the range of incidence angles expected. The mirrors consist of a 15 mm-thick fused silica substrate with a 185 mm by 30 mm area coated with a 30 nm nickel layer. The clear aperture was defined as the central 178 mm by 15 mm area on the mirror. The nickel coating also contains a small percentage of vanadium (approximately 8% atomic), which allows the coating to be more easily deposited. The coating will be referred to as NiV from now onwards.

Figure 2 shows the ideal calculated reflectivity of a NiV mirror over an x-ray energy range of 100–600 eV and the range of expected grazing incidence angles (3.75°–5.25°). The NiV optical constants used in the calculations were taken from the Center for X-Ray Optics (CXRO) database.[7]

The variation of reflectivity as a function of angle leads to a variation in the brightness across a recorded image. This variation is however small and can be taken into account by

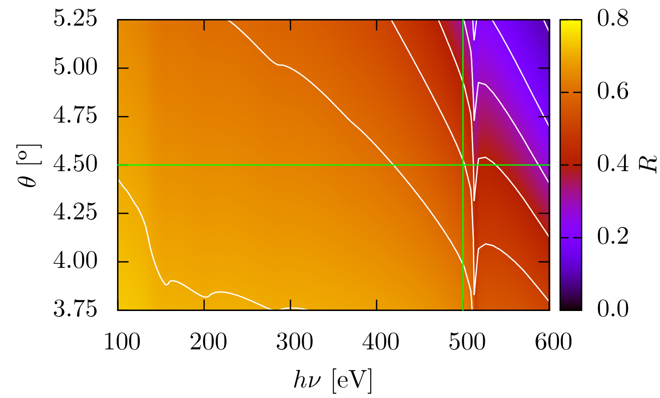

FIG. 2. Reflectivity against grazing angle and photon energy for a 92% Ni + 8% V mirror. Contours are drawn at intervals of 0.1 in reflectivity.

relating the positions of points on the image on the photocathode to a specific angle of reflection from the mirror (and hence a specific value of reflectivity taken from Figure 2) using a simple ray trace calculation. There will also be a variation of the photocathode's quantum efficiency over an image and this is also folded in with the varying mirror reflectivity.

The substrates and coatings were designed by the LLNL X-ray Science and Technology group. The substrates were polished at the Optic Shop at LLNL. The spatial resolution needed, combined with the optical design of the diagnostic, determined the required figure error for the uncoated substrates which amounted to a sphere in the 500–1000 nm peak-to-valley range (at 633 nm). The mid- and high spatial frequency surface roughness prior to coating was better than 0.75 nm rms for all the substrates.

The NiV mirror coatings were performed by means of RF magnetron sputtering at the CXRO deposition system at Lawrence Berkeley National Laboratory (LBNL). Using Rutherford backscattering measurements, the atomic composition of the NiV coating was found to be 91.8% nickel and 8.2% vanadium and the density 8.37 g/cm^3. The high spatial frequency roughness of the NiV coating (deposited on silicon wafer substrates with near-zero roughness) was 0.1 nm rms, as determined by atomic force microscopy measurements at LLNL.

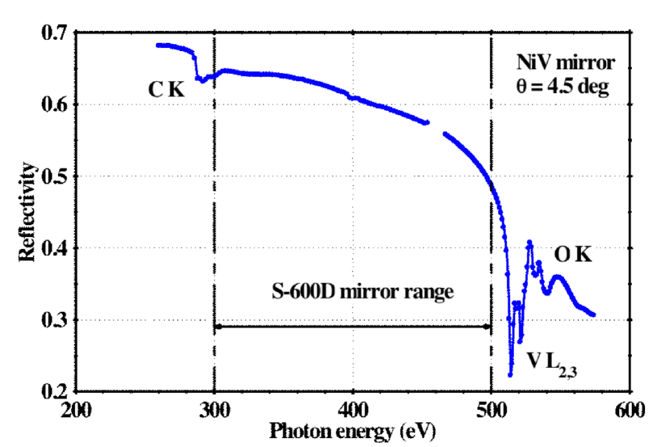

FIG. 3. Reflectivity measurements obtained at ALS on a representative NiV-coated mirror with key absorption features highlighted.

In Figure 3 we show representative reflectivity measurements taken shortly after deposition of the NiV coating on one of the mirrors, at beamline 6.3.2.[6] of the Advanced Light Source (ALS) at LBNL. Fine structure due to the vanadium $L_{2,3}$ absorption edge can be seen prominently in the measurements. The presence of the carbon and oxygen K absorption edges is mostly attributed to the presence of oxide and hydrocarbon contamination on the coating surface. Using additional measurements at ALS, the thickness uniformity of the NiV coating was found to be 0.5 nm peak-to-valley across the central 150 mm of the mirror.

B. Filters

The S600-D is compatible with a standard dimension NIF kinematic filter holder and can be fielded with a wide range of filter materials. Two filter frames are available: a "full-aperture" frame which provides uniform filtering across both images and a "half-aperture" frame which allows different filter materials and thicknesses for each image. The filter material is held in the center of the frame. An image plate with a central aperture is located on the opposite side of the frame. The image plate, typically FujiBAS-TR or -SR,[8] records a time-integrated image of the top and bottom portions of the x-ray beam(s), which fall outside the narrow DISC field of view. The purpose of the image plate is to confirm the pointing of the diagnostic post-shot and/or act as a failure diagnostic.

Two filter materials have been fielded to date with the S600-D: 1 and 2 μm thick vanadium and 0.65 μm silver layered onto 0.65 μm titanium. Figure 4 shows the band pass and transmission of each filter material when folded with the mirror response at an angle of 4.5°.

C. Aperture slit widths

The S600-D was designed for use with two different aperture slit widths: 15 μm and 45 μm. In the two-channel version three different nosecones exist, "wide/wide" (45 μm aperture in both channels), "narrow/narrow" (15 μm in both), and "narrow/wide" (one 15 μm and the other 45 μm). These two aperture widths were chosen to allow images to be recorded

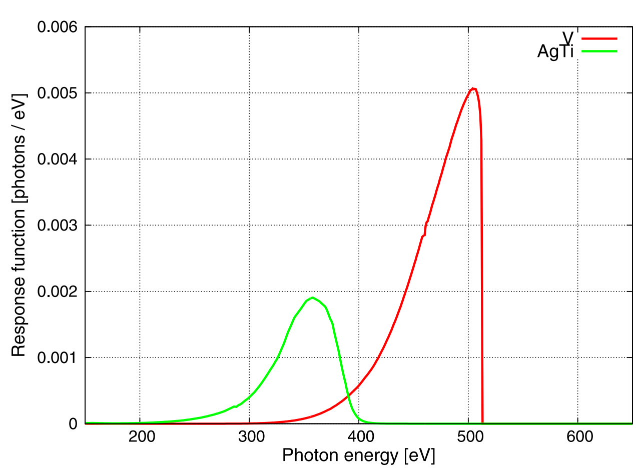

FIG. 4. Response function of each filter material used in the S600-D for a 4.5° incident angle. The vanadium filter response shown is for a thickness of 2 μm.

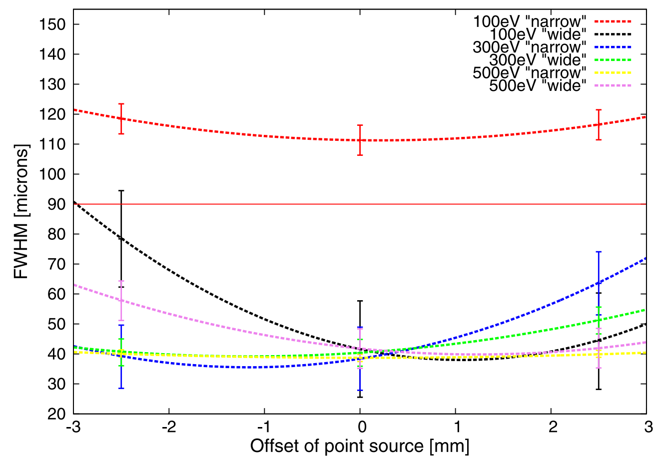

FIG. 5. Calculated resolution of the S600-D using both aperture widths, for a point source at a range of photon energies and locations relative to the central axis of the diagnostic. A simple quadratic fit was used to interpolate between the calculated values. The solid red line illustrates the limit of the required resolution.

over a range of brightnesses (especially when combined with filters of differing thicknesses).

The results of high-fidelity ray trace simulations for each aperture at a range of photon energies show that the spatial resolution of the 15 μm "narrow" slit is smaller at higher energies, but then begins to increase above that of the 45 μm "wide" aperture as the x-ray energies drop below 300 eV and diffraction effects begin to become significant. The resolution at energies below ≈200 eV for the 15 μm aperture is poorer than the 90 μm FWHM required, but this is below the region of interest for planned HED experiments using this diagnostic. Figure 5 illustrates the results of these calculations.

III. DIAGNOSTIC PERFORMANCE

To verify the operation of the imager and to measure the signal recorded in order to better tune the filtering for future experiments, two dedicated NIF shots were fielded. The first (N150520-002) involved the irradiation of an inverted L-shaped quartz wire, using a stepped 10 ns laser pulse, with 16 beams striking the horizontal wire piece and 16 striking the vertical. Titanium deposits were present on the wire, covering 3 mm on the vertical piece, imaged by the one-channel S600-D in the equatorial DIM; and 1 mm on the horizontal, imaged by the two-channel version in the polar DIM. The spacing and pattern of the deposits were designed to allow the spatial resolution of the diagnostic to be determined.

The second shot (N150521-002) used a Pleiades HED physics target.[9,10] The Pleiades platform consists of a vacuum gold half-hohlraum ("halfraum") attached to a gold cylinder containing a foam material under observation. 80 beams from the lower hemisphere of NIF deliver ≈360 kJ of laser energy to the halfraum over 2.5 ns, which in turn generates an x-ray drive which propagates into and through the foam in the cylinder. The radiation flow through the foam as a function of time is imaged in the equatorial DIM via x-ray emission from a 1.8 mm long side slot in the cylinder. The radiation

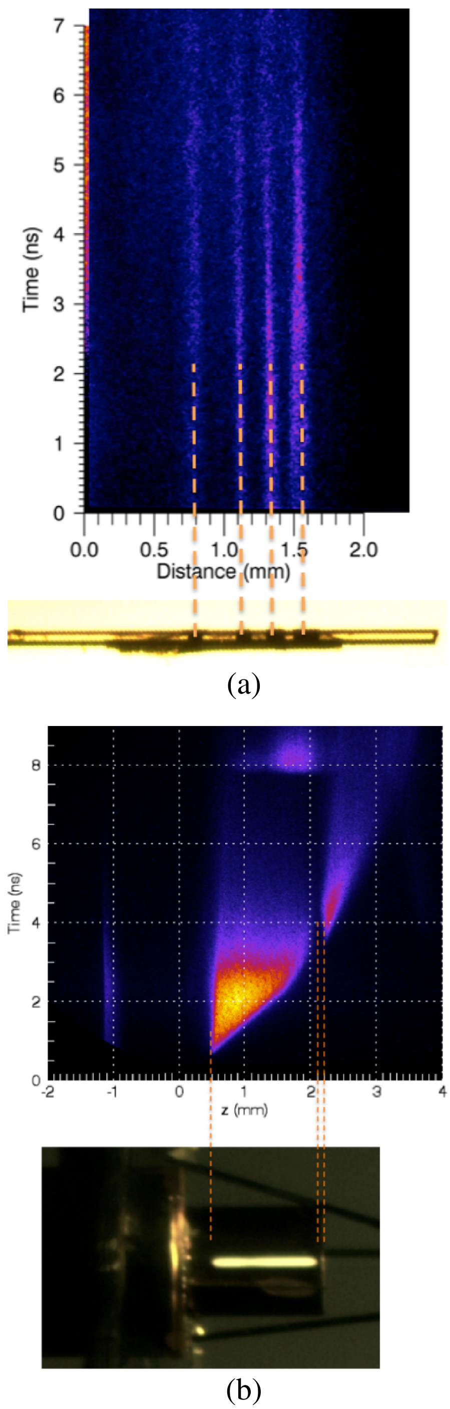

FIG. 6. Data recorded via the S600-D diagnostic. (a) Polar image taken on the wire (N150520-002) experiment using the two-channel version (only one channel shown). (b) Equatorial, single-channel image taken on the Pleiades HED (N150521-002) experiment. The propagation of radiation along the foam tube can be observed through the side slot present in the target.

is also measured via the polar DIM as it is emitted through a 100 μm by 1.5 mm slot in a zinc shield which is placed over the end of the foam tube at the opposite end of the cylinder to the halfraum.

On both shots, the one-channel configuration was fielded in the equatorial DIM and the two-channel in the pole. Figure 6 shows the data recorded alongside key features of the target for the two-channel case on the wire shot and the one-channel case on the Pleiades shot.

The polar DISC used to record the two-channel data used film as its recording medium. The corresponding imager used 15 and 45 μm aperture slits with 2 μm vanadium filtering. The same filter material was chosen for both channels on these initial shots in order to better determine the photometrics of the imager within a particular energy range. On future shots, different filter materials will be employed in each channel in order to span a greater range of the x-ray energy spectrum and perform "two-color" measurements of an emission source. The emission recorded from the titanium deposits showed that the FWHM spatial resolution was less than the 90 μm required. The equatorial DISC used a CCD as its recording medium. The imager combined a 45 μm slit with 2 μm vanadium filtering.

IV. SUMMARY

A new streaked soft x-ray imager has been developed for use on HED physics experiments on the NIF: the S600-D. This new diagnostic uses a combination of soft x-ray filters and grazing angle reflection from a nickel mirror to provide narrow band passes with FWHMs of 50 eV at energies below 510 eV. A number of qualification shots have been successfully performed which have validated the design of the S600-D against its original physics objectives.

ACKNOWLEDGMENTS

The authors thank the NIF operations team for their work in delivering the verification shots described in this paper. Thanks are also due to the LLE machinists that worked on the production of the S600-D snouts and to J. Alameda (LLNL) and J. Meyer-Ilse (LBNL) for their work on the mirror coating. This work was supported by the UK Ministry of Defence, Los Alamos National Laboratory, Laboratory for Laser Energetics, Lawrence Berkeley National Laboratory, and was performed under the auspices of the U.S. Department of Energy by Lawrence Livermore National Laboratory under Contract No. DE-AC52-07NA27344.

[1] T. M. Guymer *et al.*, Phys. Plasmas **22**, 043303 (2015).
[2] T. M. Guymer *et al.*, High Energy Density Phys. **9**, 167–171 (2013).
[3] A. S. Moore *et al.*, Rev. Sci. Instrum. **83**, 10E132 (2012).
[4] J. R. Kimbrough *et al.*, Rev. Sci. Intrum. **72**, 748 (2001).
[5] W. J. Hibbard *et al.*, Rev. Sci. Instrum. **72**, 530 (2001).
[6] E. M. Gullikson *et al.*, Proc. SPIE **4343**, 363–373 (2001).
[7] B. L. Henke *et al.*, At. Data Nucl. Data Tables **54**, 181–342 (1993).
[8] A. L. Meadowcroft *et al.*, Rev. Sci. Instrum. **79**, 113102 (2008).
[9] A. S. Moore *et al.*, J. Quant. Spectrosc. Radiat. Transfer **159**, 19–28 (2015).
[10] C. L. Fryer *et al.*, High Energy Density Phys. **18**, 45–54 (2016).